2021 European Control Conference (ECC)
June 29 - July 2, 2021. Rotterdam, Netherlands

An Adaptive Observer approach to Slip Estimation for Agricultural Tracked Vehicles

Roberto Tazzari[1], Ilario A. Azzollini[1] and Lorenzo Marconi[1]

***Abstract*— The paper deals with autonomous Unmanned Ground Vehicles developed for precision agriculture contexts. The focus of the paper is on the design of an adaptive observer for slip estimation ensuring exponential convergence to the real slip coefficients. Uniform global exponential stability of the origin of the error system is shown via Lyapunov analysis and persistency of excitation arguments. Furthermore, robustness to additive perturbations is shown in terms of Input-to-State Stability. Experimental results validate the effectiveness of the proposed estimator even in presence of noisy measurements.**

***Index Terms*— Adaptive observer, agricultural robotics, persistency of excitation, slip estimation, tracked vehicle.**

I. INTRODUCTION

Mobile robotics in outdoor applications is already widespread in several fields [1]–[4]. Recently, also agriculture, namely Precision Agriculture (PA), is merging farming techniques with data science and robotics to optimize farming processes [5], [6] and to support farmer decisions. Currently, PA autonomous platforms are mostly deployed in *open-field* farming, while for Orchard PA (OPA) they are still at research level. The main difference between the two lies in the navigation. In open field, GPS data are enough to reliably navigate, while trees canopy and orchard structure can obstruct GPS signals requiring GPS-free navigation strategies. This work frames within the latter scenario and, in line with [7]–[9], robot localization is achieved by leveraging odometry, LiDAR, and Inertia Measurement Unit (IMU).

Caterpillars feature a wider contact surface with the ground if compared to wheels, with a higher level of traction and stability. Therefore, they are the ideal choice for Unmanned Ground Vehicle (UGV) designed for rough terrains [10]. The main drawback of this locomotion system lies in the turning mechanism. In fact, the two tracks are actuated with different velocities causing the robot to skid over the ground - from here the name Skid-Steering Vehicles (SSVs) - shearing the terrain as in Fig. 1. This slip reduces the reliability of odometry, making slip estimation even more relevant for localization and navigation purposes. Accurate slip estimation is also relevant for OPA tasks, as a good estimate of the vehicle velocity and position increases the capability of keeping a constant working speed, which is a key requirement in most of orchard operations, e.g. spraying.

Ideally, a SSV should behave as a Differential Wheeled Robot (DWR) but the presence of slip creates a mismatch between the two systems. This difference makes the problem

Fig. 1: Terrain shearing during turning maneuvers.

of path following for tracked vehicles more complex and motivated several research activities aiming to design algorithms for estimating/compensating this effect. In particular, the kinematic slip has been modeled as a constant plus an additive zero-mean stochastic process and then estimated using Kalman filters as in [11]–[14] or adaptively [15]. On the other hand, [16], [17] studied the relation between the slip and track speeds, remarking the dependence of the slip on track velocities, turning radius and soil properties. However, these relations work only when the turning radius is kept small enough. Differently from all the other approaches, [18], [19] were driven by data fitting, leading to the definition of ad hoc slip models tailored for the specific platform-terrain combination considered.

Focusing on adaptive approaches, [15] models the slip as a random walk, estimating it through a recursive least squares and then using it to adapt the control action considering a DWR-based reference model, following a direct model reference adaptive control approach. Instead, [20] designs an adaptive feedback linearization control for the dynamic model of a wheeled SSV. We observe that, in line with classic adaptive control literature, both [15] and [20] share the need of Persistency of Excitation (PE) conditions in order to have convergence of the slip estimates to the true slip coefficients, without discussing in details what this would mean in terms of mobile robot trajectories.

In this paper, we propose an adaptive observer which robustly estimates the slip coefficients with an exponential convergence rate, assuming the UGV moves at constant linear and angular velocities. This assumption is in line with the typical navigation trajectories required to be performed by an orchard agriculture robot. In particular, we design our estimator by mixing an identity observer with classic adaptive laws, the latter found via a Lyapunov analysis. The design choice is convenient to bring the error system

[1]Roberto Tazzari, Ilario A. Azzollini and Lorenzo Marconi are with CASY-DEI, University of Bologna (roberto.tazzari2@unibo.it, ilario.azzollini@unibo.it and lorenzo.marconi@unibo.it).

in a standard form [21]. Moreover, in contrast to existing adaptive approaches [15], [20], we formally prove how the considered trajectories are persistently exciting for our estimator, resulting in a globally uniformly exponentially stable origin for the estimation error system.

Notation: We denote by $\mathbb{R}$ the set of real numbers and we define $\mathbb{R}_{\geq 0} := [0, \infty)$. $\|\cdot\|$ denotes the Euclidian norm of vectors and induced norm of matrices, while $\|\cdot\|_p$, with $p \in [1, \infty]$, indicates the $\mathcal{L}_p$ norm of time signals. In particular, for a measurable function $\phi : \mathbb{R}_{\geq 0} \to \mathbb{R}^n$, $\|\phi\|_p := (\int_{t_0}^{\infty} \|\phi(t)\|^p \ dt)^{1/p}$ for $p \in [1, \infty)$, and $\|\phi\|_\infty := \text{ess sup}_{t \geq t_0} \|\phi(t)\|$. For $c_r > 0$, B_{c_r} denotes the open ball $B_{c_r} := \{x \in \mathbb{R}^n : \|x\| < c_r\}$. A function $\gamma : \mathbb{R}_{\geq 0} \to \mathbb{R}_{\geq 0}$ belongs to *class-*$\mathcal{K}$ ($\gamma \in \mathcal{K}$) if it is continuous, strictly increasing and $\gamma(0) = 0$. Moreover, if in addition $\gamma(s) \to_{s \to \infty} \infty$, γ is said to belong to *class-*$\mathcal{K}_\infty$ ($\gamma \in \mathcal{K}_\infty$). A solution to the differential equation $\dot{x} = f(t, x)$ at time t with initial conditions $(t_0, x_0) \in \mathbb{R}_{\geq 0} \times \mathbb{R}^n$ is denoted as $(x(t, t_0, x_0))$, or simply $x(t)$. For the function $V : \mathbb{R}_{\geq 0} \times \mathbb{R}^n \to \mathbb{R}$, we define $\dot{V}_{(\#)}(t, x) := (\partial V/\partial t) + (\partial V/\partial x) f(t, x)$ where $(\#)$ denotes the equation number that labels equation $\dot{x} = f(t, x)$.

II. MODELS

SSV kinematic model: Under the main assumption of planar motion, we consider the following kinematic model, described with respect to an inertial reference frame $\mathcal{F}_i(O_i, x, y, z)$, as

$$\begin{aligned} \dot{x} &= V_G \cos\theta \\ \dot{y} &= V_G \sin\theta \\ \dot{\theta} &= \Omega_z \end{aligned} \tag{1}$$

where V_G is the linear velocity of the Center of Gravity (CoG) in body coordinates, $\mathcal{F}_b(O_b, x_b, y_b, z_b)$, and Ω_z represents the angular velocity of the vehicle around the axis normal to the motion plane. The main quantities of interest are also presented in Fig. 2. Both SSVs and DWRs kinematics can be described using (1), due to their nonholonomic nature. The main difference lies in the expressions of V_G and Ω_z. In fact, for DWRs they can be computed as

$$\begin{aligned} V_G &= \frac{v_R + v_L}{2} = \frac{r}{2}(\omega_R + \omega_L) \\ \Omega_z &= \frac{v_R - v_L}{2d} = \frac{r}{2d}(\omega_R - \omega_L) \end{aligned} \tag{2}$$

while for SSVs the same quantities are expressed as

$$\begin{aligned} V_G &= \frac{v_R(1 - i_R(t)) + v_L(1 - i_L(t))}{2} \\ &= \frac{r}{2}(\omega_R(1 - i_R(t)) + \omega_L(1 - i_L(t))) \\ \Omega_z &= \frac{v_R(1 - i_R(t)) - v_L(1 - i_L(t))}{2d} \\ &= \frac{r}{2d}(\omega_R(1 - i_R(t)) - \omega_L(1 - i_L(t))). \end{aligned} \tag{3}$$

The quantities ω_R, ω_L are the right and left angular motor speeds, respectively, and similarly, v_R, v_L represent the linear velocities of the right and left wheel (or track). The quantity

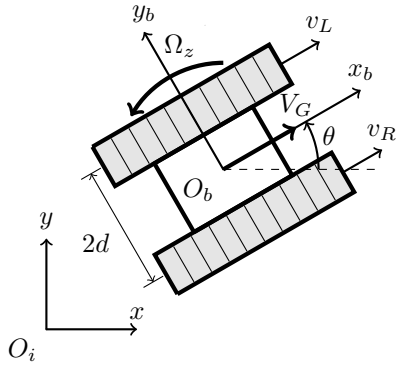

Fig. 2: Planar motion of a tracked vehicle.

r is the wheel (or track sprocket) radius, while d is half the distance between the center lines passing through the two wheels (or tracks), also shown in Fig. 2.

The difference between (2) and (3) is given by the presence of $i_R(t), i_L(t) \in (-1, 1)$ that are the time-varying slip coefficients associated with the right and left track, respectively. Notice that in (3), the real inputs driving the system are $(1 - i_R)v_R$ and $(1 - i_L)v_L$, resulting in a variation of the efficiency of the control inputs v_L, v_R. By letting

$$\begin{cases} \eta_R & := 1 - i_R, \qquad 0 < \eta_R < 2 \\ \eta_L & := 1 - i_L, \qquad 0 < \eta_L < 2 \end{cases} \tag{4}$$

the overall kinematic model (1) is rewritten as

$$\begin{aligned} \dot{x} &= \frac{\eta_R \cos\theta}{2} v_R + \frac{\eta_L \cos\theta}{2} v_L \\ \dot{y} &= \frac{\eta_R \sin\theta}{2} v_R + \frac{\eta_L \sin\theta}{2} v_L \\ \dot{\theta} &= \frac{\eta_R}{2d} v_R - \frac{\eta_L}{2d} v_L \ , \end{aligned} \tag{5}$$

which is a system with control inputs v_R, v_L, and exogenous (uncontrollable) inputs η_R, η_L.

Slip coefficients model: While it is a well-known fact [16], [17], [22], [23] that i_R, i_L depend on the soil type as well as on the track velocities (both absolute and relative to each other), to the best of authors' knowledge, a mathematical model capturing the underlying complex relation is not available in literature.

In [16] and [17], it is observed that there is a nonlinear relation between the ratio $i_R(t)/i_L(t)$ and v_R, v_L but this result is limited to small turning radii, and a complete relation also including soil dependency is still missing. In general, track slip coefficients are expressed as

$$i = 1 - \frac{V_t}{v_i} = 1 - \frac{V_t}{\omega r} \tag{6}$$

where i is the slip coefficient of a track, v_i is the ideal velocity of the track given by the product of the driving sprocket rotational speed ω and its radius r, and V_t is the actual speed of the track-ground contact point (which is hardly measurable). Equation (6) shows the relation between the value of the slip coefficient and the track velocity, but it does not show any dependency on soil-related parameters.

On the other hand, [22] and [23] report a relation between slip coefficients and the traction force of the track to the ground, which depends on the physical properties of the terrain according to

$$F = F_{max}\left[1 - \frac{K}{il}\left(1 - e^{-il/K}\right)\right] \tag{7}$$

where l is the length of the contact surface between the track and the ground, K represents the soil shear deformation modulus and F_{max} is the maximum traction force developed by a track. The latter can be expressed as

$$F_{max} = S_c\tau_{max} = S_c\left(c + p\tan\varphi\right) = S_c c + \frac{W}{2}\tan\varphi$$

in which S_c is the track-ground contact surface, τ_{max} the maximum shear strength of the terrain, c the apparent cohesion of the terrain and φ the angle of internal shearing resistance of the soil, p is the normal pressure acting on the track and W the total weight of the vehicle. Inverting (7) it is then possible to retrieve the slip coefficient of the track, given soil parameters and the traction forces applied by each of them, as done in [24]. Once again, the relation found is incomplete, as it does not relate both track velocities and soil features in a single equation.

In conclusion, both (6) and (7) are incomplete and therefore there is no advantage in considering the dynamic model over the kinematic one for problems of slip estimation.

III. PROBLEM STATEMENT

The following general problem is considered.

Problem 1 *Considering system* (5)*, the problem at hand is to design a dynamical system with inputs x, y, θ, v_R, v_L, producing as output the estimates $\hat{\eta}_R$, $\hat{\eta}_L$ asymptotically converging to the true coefficients η_R and η_L, respectively.*

As emphasized previously, the general problem is hard to be solved as it would require a model relating the intrinsically time-varying slip coefficients to the system states and inputs, as well as to the time-varying (and practically impossible to be modeled or measured) terrain parameters. The application framework given by OPA leads to simplifying assumptions making the problem more tractable, as most of the farming tasks require to navigate the orchard at a constant speed.

Orchard works feature a repetitive pattern in which one has to travel along the field lane, then switch to the following one, and so on. Therefore, it is possible to define two different navigation scenarios:

- *Straight motion* - navigating the current orchard row at a constant speed;
- *Turning motion* - switching from the current row to the next one at constant speed and turning radius.

While for straight motion constant speed is required by the tasks themselves (e.g to uniformly spray pesticides), for turning motion it is simply the most efficient trajectory for SSVs. In [7], where car-like vehicles are considered, it is shown that particular techniques have to be adopted for lane-switching manoeuvres, being turning radii bounded by their steering capabilities. Differently, SSVs allow one to perform turning manoeuvres with small turning radius (even zero).

Notice that each scenario requires the robot to move at a constant V_G and Ω_Z, which are obtained, according to (2), from constant values of v_R, v_L. From (6), it is possible to claim that when v_i is constant, i is constant as well. On the other hand, provided that constant track velocities are given by constant track forces, (7) requires the terrain to be homogeneous in order to obtain constant coefficients, which is a reasonable assumption in OPA. Then, this application framework allows one to rewrite the coefficients $i_R(t)$ and $i_L(t)$ as constants, namely $i_R(t) = i_R$ and $i_L(t) = i_L$. We want to comment already at this point that these considerations are validated by all the experimental results we performed on the field (as described in Section V). Formally, the problem is considered under the following assumption.

Assumption 1 *The linear velocities v_R, v_L in* (5) *are constant and positive. Moreover, the soil is homogeneous, therefore also i_R, i_L are constant.*

IV. MAIN RESULT

Assuming that x, y, θ, v_R, v_L can be measured, the proposed estimator is the *adaptive identity observer*:

$$\begin{bmatrix}\dot{\hat{x}}\\ \dot{\hat{y}}\\ \dot{\hat{\theta}}\end{bmatrix} = \begin{bmatrix}\frac{\cos\theta}{2}v_R & \frac{\cos\theta}{2}v_L\\ \frac{\sin\theta}{2}v_R & \frac{\sin\theta}{2}v_L\\ \frac{1}{2d}v_R & -\frac{1}{2d}v_L\end{bmatrix}\begin{bmatrix}\hat{\eta}_R\\ \hat{\eta}_L\end{bmatrix} + \underbrace{\begin{bmatrix}l_1 & 0 & 0\\ 0 & l_2 & 0\\ 0 & 0 & l_3\end{bmatrix}}_{L}\begin{bmatrix}e_x\\ e_y\\ e_\theta\end{bmatrix}$$
$$\begin{bmatrix}\dot{\hat{\eta}}_R\\ \dot{\hat{\eta}}_L\end{bmatrix} = \underbrace{\begin{bmatrix}\lambda_1 & 0\\ 0 & \lambda_2\end{bmatrix}}_{\Lambda}\begin{bmatrix}\frac{\cos\theta}{2}v_R & \frac{\sin\theta}{2}v_R & \frac{1}{2d}v_R\\ \frac{\cos\theta}{2}v_L & \frac{\sin\theta}{2}v_L & -\frac{1}{2d}v_L\end{bmatrix}\begin{bmatrix}e_x\\ e_y\\ e_\theta\end{bmatrix} \tag{8}$$

where the state $\begin{bmatrix}\hat{x} & \hat{y} & \hat{\theta} & \hat{\eta}_R & \hat{\eta}_L\end{bmatrix}^\top \in \mathbb{R}^5$ contains the estimates of $x, y, \theta, \eta_R, \eta_L$ in (5), the output-injection matrix $L \in \mathbb{R}^{3\times 3}$ and the adaptive-gain matrix $\Lambda \in \mathbb{R}^{2\times 2}$ are design parameters to be chosen, and we define the *observation error*

$$e = \begin{bmatrix}e_x\\ e_y\\ e_\theta\end{bmatrix} = \begin{bmatrix}x - \hat{x}\\ y - \hat{y}\\ \theta - \hat{\theta}\end{bmatrix}. \tag{9}$$

The properties of the estimator are presented in the following theorem, which represents the main result of this work.

Theorem 1 *Under Assumption 1, the problem of slip coefficients estimation is solved by the adaptive observer* (8) *with arbitrary initial conditions, and with L and Λ positive definite. In particular, the estimator guarantees uniform exponential convergence of the estimates to the true slip coefficients as time goes to infinity: $\hat{\eta}_R \to \eta_R$, $\hat{\eta}_L \to \eta_L$.*

Proof: We change coordinates by considering the observation error, (9), along with the *estimation error*

$$\tilde{\eta} = \begin{bmatrix}\tilde{\eta}_R\\ \tilde{\eta}_L\end{bmatrix} = \begin{bmatrix}\hat{\eta}_R - \eta_R\\ \hat{\eta}_L - \eta_L\end{bmatrix}.$$

Thus, system (8) in the new error coordinates becomes

$$\dot{\varepsilon} = \begin{bmatrix} \dot{e} \\ \dot{\tilde{\eta}} \end{bmatrix} = \begin{bmatrix} -L & \Phi^\top(t) \\ -\Lambda\Phi(t) & 0 \end{bmatrix} \begin{bmatrix} e \\ \tilde{\eta} \end{bmatrix} = A(t,\varepsilon) \tag{10}$$

where, we call *regressor* the matrix

$$\Phi(t) = \begin{bmatrix} -\frac{\cos\theta(t)}{2} v_R & -\frac{\sin\theta(t)}{2} v_R & -\frac{1}{2d} v_R \\ -\frac{\cos\theta(t)}{2} v_L & -\frac{\sin\theta(t)}{2} v_L & \frac{1}{2d} v_L \end{bmatrix}. \tag{11}$$

System (10) is almost standard in adaptive control literature, with the peculiarity of having a matrix regressor, instead of just a vector. Solving our problem is equivalent to conclude uniform global asymptotic stability of the origin for the error system (error system 0-UGAS). To treat our problem we rely on Corollary 1 and Theorem 2 of [21]. These results require two assumptions (A1, A2) to hold, as well as requiring the pair (Φ, A) to be uniformly persistently exciting (u-PE).

A1 [21] *There exist $\gamma_1 \in \mathcal{K}_\infty$, a locally bounded function $\gamma_2 : \mathbb{R}_{\geq 0} \to \mathbb{R}_{\geq 0}$ and a positive definite continuous function $\gamma_3 : \mathbb{R}_{\geq 0} \to \mathbb{R}_{\geq 0}$, such that for all (t_0, ε_0), all corresponding solutions of* (10) *satisfy*

$$\begin{aligned} \|\varepsilon\|_\infty &\leq \gamma_1(\|\varepsilon_0\|) \\ \|\gamma_3(\|e\|)\|_1 &\leq \gamma_2(\|\varepsilon_0\|). \end{aligned} \tag{12}$$

From [21, Remark 4] we know that A1 is satisfied if, for instance, there exist a locally Lipschitz function V and two functions $\underline{\alpha}, \overline{\alpha} \in \mathcal{K}_\infty$ such that

$$\begin{aligned} \underline{\alpha}(\|\varepsilon\|) \leq V(t,\varepsilon) &\leq \overline{\alpha}(\|\varepsilon\|) \\ \dot{V}_{(10)}(t,\varepsilon) &\leq -\gamma_3(\|e\|). \end{aligned}$$

To prove this, we consider the Lyapunov function candidate

$$V(\varepsilon) = \frac{1}{2}\left(e^\top L^{-1} e + \tilde{\eta}^\top \Lambda^{-1} \tilde{\eta}\right)$$

which is a valid candidate by choosing $l_1 > 0$, $l_2 > 0$, $l_3 > 0$, $\lambda_1 > 0$, $\lambda_2 > 0$, as stated in Theorem 1. Now, its time derivative along the error system trajectories is

$$\begin{aligned} \dot{V}_{(10)}(\varepsilon) &= -e^\top e + e^\top \Phi^\top \tilde{\eta} - \tilde{\eta}^\top \Phi e \\ &= -\|e(t)\|^2 = -\gamma_3(\|e\|) \end{aligned} \tag{13}$$

which is negative semidefinite. In addition, each entry of the regressor $\Phi(t)$ is bounded and globally Lipschitz. Therefore, by La Salle/Yoshizawa [25, Theorem 8.4], system (10) is 0-UGS and

$$\lim_{t\to\infty} \|e(t)\|^2 = 0$$

resulting in $e(t) \to 0$, satisfying A1. In fact, we can introduce $c_m, c_M > 0$ such that

$$\underline{\alpha}(\|\varepsilon\|) = c_m^2 \|\varepsilon\|^2 \leq V(\varepsilon) \leq c_M^2 \|\varepsilon\|^2 = \overline{\alpha}(\|\varepsilon\|).$$

Moreover, being $V(\varepsilon)$ a positive nonincreasing function bounded from below by 0, we conclude that it has a limit

$$\lim_{t\to\infty} V(t) = V_\infty.$$

Integrating (13) from t_0 to ∞, it results

$$\int_{t_0}^{\infty} \|e(\tau)\|^2 \, d\tau = -\int_{t_0}^{\infty} \dot{V}(\tau) \, d\tau = V(\varepsilon_0) - V_\infty$$

and we have

$$V(\varepsilon_0) - V_\infty \leq V(\varepsilon_0) \leq c_M^2 \|\varepsilon_0\|^2 = \gamma_2(\|\varepsilon_0\|).$$

Also,

$$c_m^2 \|\varepsilon\|_\infty^2 \leq c_m^2 \|\varepsilon(t)\|^2 \leq V(\varepsilon(t)) \leq V(\varepsilon_0) \leq c_M^2 \|\varepsilon_0\|^2$$

from which $\|\varepsilon\|_\infty \leq (c_M/c_m)\|\varepsilon_0\|$. Thus (12) holds with $\gamma_1(s) = (c_M/c_m)s$, $\gamma_2(s) = c_M^2 s^2$ and $\gamma_3(s) = s^2$.

A2 [21] *Each entry of Φ is locally Lipschitz, and there exist nondecreasing functions $\rho_i : \mathbb{R}_{\geq 0} \to \mathbb{R}_{\geq 0}$, $(i = 1, 2, 3)$ such that, for almost all $(t, \varepsilon) \in \mathbb{R}_{\geq 0} \times \mathbb{R}^5$*

$$\begin{aligned} \max\{\|Le\|, \|\Lambda\Phi e\|\} &\leq \rho_1(\|\varepsilon\|)\|e\| \\ \|\Phi\| &\leq \rho_2(\|\varepsilon\|) \\ \left\|\frac{\partial\Phi}{\partial t}\right\| &\leq \rho_3(\|\varepsilon\|). \end{aligned}$$

Being the entries of our regressor bounded and globally Lipschitz, A2 trivially holds with some constants ρ_1, ρ_2, ρ_3.

Definition: u-PE [21] *The pair (Φ, A) is called uniformly persistently exciting (u-PE) if, for each $c_r > 0$, there exist $\mu, T > 0$, such that, for all $(t_0, \varepsilon_0) \in \mathbb{R}_{\geq 0} \times B_{c_r}$, all corresponding solutions satisfy*

$$\int_t^{t+T} \Phi(\tau)\Phi^\top(\tau) \, d\tau \geq \mu I \quad \forall t \geq t_0. \tag{14}$$

In general it is difficult to check the u-PE condition since it must be valid for all possible solutions, clearly impossible to be known a priori. However, the proposed design leads to

$$\Phi\Phi^T = \begin{bmatrix} \frac{v_R^2}{4}\left(1 + \frac{1}{d^2}\right) & \frac{v_R v_L}{4}\left(1 - \frac{1}{d^2}\right) \\ \frac{v_R v_L}{4}\left(1 - \frac{1}{d^2}\right) & \frac{v_L^2}{4}\left(1 + \frac{1}{d^2}\right) \end{bmatrix}$$

which is positive definite for any positive v_R, v_L. In particular, it is even constant and positive definite under Assumption 1, and, as a consequence, (14) is directly satisfied in both scenarios. Under A1, A2 and having u-PE, we conclude that the error system (10) is 0-UGAS [21, Corollary 1].

Moreover, by [21, Theorem 2] we conclude 0-UGES as: (i) $\Phi(t)$ is independent of ε; (ii) $\gamma_1(s)$, $\gamma_2(s)$, $\gamma_3(s)$ are proportional to s, s^2, and s^2, respectively, for all s. ■

Remark 1 *The extra requirement given by the u-PE property does not only guarantee convergence to the true parameters, but it also guarantees robustness for the error system* (10) *with respect to additive perturbations (i.e. considering $\dot{\varepsilon} = A(t,\varepsilon) + d(t)$). In particular, when the u-PE contributes to conclude uniform global asymptotic stability, the error system is "totally stable", which means it is robust against "small" nonvanishing perturbations [21, Equation (13)]. In our case, u-PE induces uniform global exponential stability, so the error system is robust with respect to arbitrarily large nonvanishing perturbations as the system is globally input-to-state stable [25, Lemma 4.6]. This property derives from a converse Lyapunov theorem [25, Theorem 4.14]. Robustness of the proposed adaptive observer is shown in Section V as*

we have real noisy measurements.
The vast majority of other designs present in the literature, explicitly or implicitly assume the slip coefficients to be constant (resulting in a zero-error result) or slowly time-varying (resulting in a small-error "practical" result). Our work is perfectly in line with these results and, in addition: (i) we discuss how only with constant track velocities and homogeneous soil it makes sense to consider constant slip coefficients; (ii) we formally prove that for any positive constant track velocities we have u-PE and related robustness. Notice that with other design choices the straight motion could result to be not u-PE [15].

Remark 2 *Oftentimes, adaptive approaches are not appealing for robotics applications as, in order to have robustness (which is induced by the u-PE property), the robot needs to perform some kind of oscillatory trajectories in order to obtain sufficiently rich signals. In contrast to this, with our design we have u-PE even for constant inputs v_R, v_L, resulting in smooth trajectories, which makes the designed estimator appealing for OPA applications.*

Remark 3 *The design of an identity observer on top of the adaptive laws may seem redundant as we are measuring the whole state. The intuition behind the proposed design comes from noticing that* (5) *is linear in the parameters to be found:*

$$\begin{bmatrix} \dot{x} & \dot{y} & \dot{\theta} \end{bmatrix}^\top = -\Phi^\top \begin{bmatrix} \eta_R & \eta_L \end{bmatrix}^\top$$

where, as already emphasized by Assumption 1, the unknown parameters η_R, η_L are constant. This is a desirable scenario for designing adaptive laws. However, as we do not have direct measurements of $\dot{x}, \dot{y}, \dot{\theta}$, we cannot design estimation laws for the unknown parameters without designing any extra dynamical system. This reasoning is what justified our choice to design an identity observer to be combined with the estimation laws. This choice resulted to be very convenient both in order to bring the error system in the standard form (10)*, and in terms of u-PE requirement.*

V. EXPERIMENTAL RESULTS

Experimental tests were performed using the agricultural tracked UGV described in details in [9] and [26]. In particular, the state measurements were provided by the onboard sensor suite. Namely, we measured x, y, θ using a high precision GNSS sensor with an embedded compass. Notice that we used raw-data measurements, without any filtering, to highlight robustness of the proposed design.

To compare the estimates of slip coefficients coming from (8) with ground truth values, we used (6) as follows:

$$\begin{aligned} i_R &= 1 - \frac{V_{t,R}}{v_R} = 1 - \frac{V_{G,m} + d\Omega_{z,m}}{v_{R,m}} \\ i_L &= 1 - \frac{V_{t,L}}{v_L} = 1 - \frac{V_{G,m} - d\Omega_{z,m}}{v_{L,m}} \end{aligned} \tag{15}$$

in which, $V_{t,R}, V_{t,L}$ are the right and left track true velocities, respectively. The subscript m identifies the measured quantities: $V_{G,m}$ from the GNSS, $\Omega_{z,m}$ from IMU data (gyroscope) and $v_{R,m}, v_{R,m}$ collected from motor encoders. For ground truth sake, we performed the experiments in open-field and not inside orchard rows, in order to obtain more accurate and reliable GNSS data.

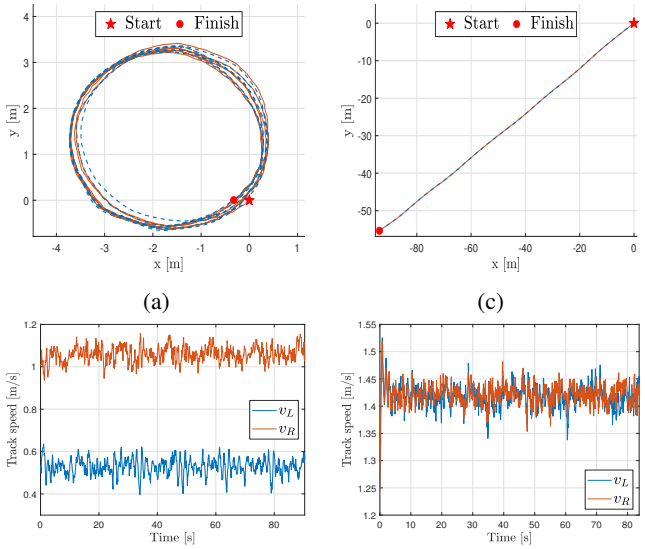

Fig. 3: Circular and straight motion experiments. (a),(c): Measured (continuous) and estimated position (dashed) trajectories. (b),(d): Corresponding track velocities.

To test the performance of (8) in both the navigation scenarios described above, we carried out experiments in which the robot negotiated: (i) a circular trajectory, as shown in Fig. 3.a with constant turning radius and angular velocity, in fact, Fig. 3.b shows noisy but constant values of v_L, v_R; (ii) a straight linear trajectory, as shown in Fig. 3.c, with constant linear body velocity, indeed, Fig. 3.d shows constant values of the two tracks velocities, highlighting the noisy nature of measurements collected.

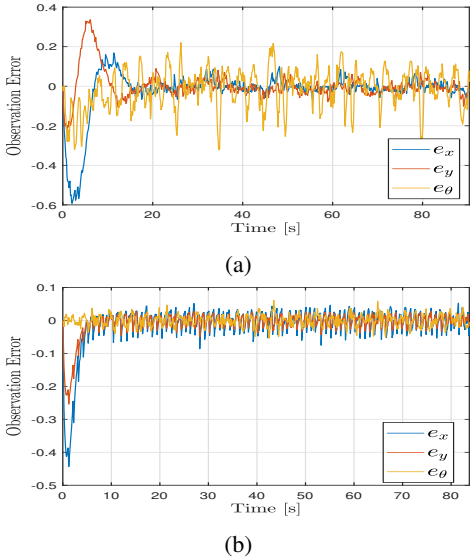

Fig. 4: Observation error (9): (a) circular and (b) straight motion.

While Fig. 3.a and Fig. 3.c qualitatively show how the

observed trajectory and the real ones tend to overlap, Fig. 4.a and Fig. 4.b give proper values of the observation errors e_x, e_y, e_θ, respectively for circular and straight motion tests. As expected from Remark 1, Fig. 5 shows the robust convergence of the estimated slip coefficients $\hat{\eta}_L, \hat{\eta}_R$, to the real ones, η_L, η_R, approximated using (4) and (15).

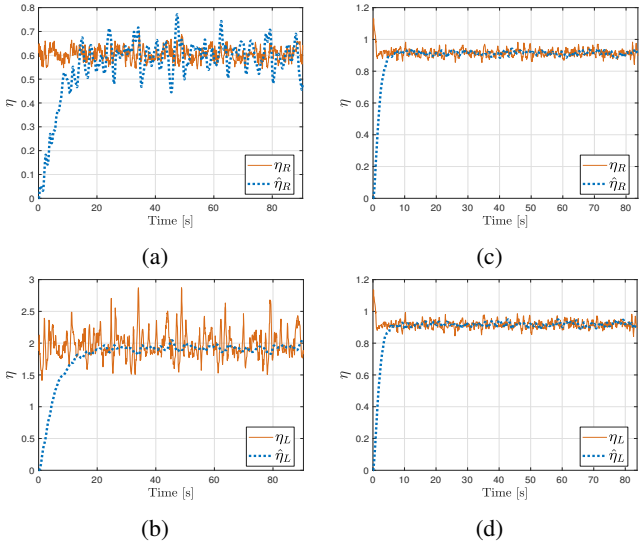

Fig. 5: Slip estimation: (a),(b) circular and (c),(d) straight motion.

It is also important to mention that the good performance obtained during experimental tests are not given by specifically-tuned observer parameters, but rather by the structural properties described and proved in Sec. IV. In fact, both L, Λ have been considered as identity matrices (this also explains the convergence time), since the focus of this paper is to show the effectiveness of the proposed approach rather than fine tuning parameters for a particular application.

VI. CONCLUSIONS

In this work, we presented an adaptive observer for slip estimation for tracked skid-steering vehicles. We formally proved uniform global exponential stability of the error system, resulting in robustness with respect to additive perturbations in terms of input-to-state stability. Experimental tests showed the good performance of the proposed approach. Future work will be devoted to use this estimator in synergy with a controller in an *indirect* adaptive control fashion.

ACKNOWLEDGMENTS

The authors would like to thank Dario Mengoli for his support during experimental tests, ASLATECH for the construction of the robot, and the "Dipartimenti d'Eccellenza" Project sposored by the Italian Ministry of University.

REFERENCES

[1] J. Delmerico, S. Mintchev *et al.*, "The current state and future outlook of rescue robotics," *Journal of Field Robotics*, vol. 36, no. 7, pp. 1171–1191, 2019.

[2] I. A. Azzollini, N. Mimmo, and L. Marconi, "An Extremum Seeking Approach to Search and Rescue Operations in Avalanches using ARVA," *IFAC-PapersOnLine*, vol. 53, no. 2, pp. 1627–1632, 2020.

[3] W. H. Chun and N. Papanikolopoulos, "Robot surveillance and security," in *Springer Handbook of Robotics*. Springer, 2016, pp. 1605–1626.

[4] K. Yoshida, "Achievements in space robotics," *IEEE Robotics & Automation Magazine*, vol. 16, no. 4, pp. 20–28, 2009.

[5] Haverkort, A.J. Ancha Srinivasan (ed), *Handbook of precision agriculture: principles and applications*. The Haworth Press Inc., 2007.

[6] D. Slaughter, D. Giles, and D. Downey, "Autonomous robotic weed control systems: A review," *Computers and electronics in agriculture*, vol. 61, no. 1, pp. 63–78, 2008.

[7] M. Bergerman, S. M. Maeta *et al.*, "Robot farmers: Autonomous orchard vehicles help tree fruit production," *IEEE Robotics & Automation Magazine*, vol. 22, no. 1, pp. 54–63, 2015.

[8] A. Costley and R. Christensen, "Landmark aided gps-denied navigation for orchards and vineyards," in *2020 IEEE/ION Position, Location and Navigation Symposium (PLANS)*, 2020, pp. 987–995.

[9] D. Mengoli, R. Tazzari, and L. Marconi, "Autonomous Robotic Platform for Precision Orchard Management: Architecture and Software Perspective," in *2020 IEEE International Workshop on Metrology for Agriculture and Forestry (MetroAgriFor)*, 2020, pp. 303–308.

[10] J. Wong and W. Huang, "Wheels vs. tracks – A fundamental evaluation from the traction perspective," *Journal of Terramechanics*, vol. 43, no. 1, pp. 27 – 42, 2006.

[11] B. Zhou, Y. Peng, and J. Han, "UKF based estimation and tracking control of nonholonomic mobile robots with slipping," in *2007 IEEE International Conference on Robotics and Biomimetics (ROBIO)*. IEEE, 2007, pp. 2058–2063.

[12] T. M. Dar and R. G. Longoria, "Slip estimation for small-scale robotic tracked vehicles," in *Proceedings of the 2010 American Control Conference*, 2010, pp. 6816–6821.

[13] F. Rogers-Marcovitz, N. Seegmiller, and A. Kelly, "Continuous vehicle slip model identification on changing terrains," in *Proceedings of RSS 2012 Workshop on Long-term Operation of Autonomous Robotic Systems in Changing Environments*, July 2012.

[14] B. Sebastian and P. Ben-Tzvi, "Active Disturbance Rejection Control for Handling Slip in Tracked Vehicle Locomotion," *Journal of Mechanisms and Robotics*, vol. 11, no. 2, 02 2019.

[15] M. Burke, "Path-following control of a velocity constrained tracked vehicle incorporating adaptive slip estimation," in *2012 IEEE International Conference on Robotics and Automation*, 05 2012, pp. 97–102.

[16] K. Nagatani, D. Endo, and K. Yoshida, "Improvement of the odometry accuracy of a crawler vehicle with consideration of slippage," in *Proceedings 2007 IEEE International Conference on Robotics and Automation*. IEEE, 2007, pp. 2752–2757.

[17] D. Endo, Y. Okada *et al.*, "Path following control for tracked vehicles based on slip-compensating odometry," in *2007 IEEE/RSJ International Conference on Intelligent Robots and Systems*. IEEE, 2007, pp. 2871–2876.

[18] S. A. A. Moosavian and A. Kalantari, "Experimental slip estimation for exact kinematics modeling and control of a tracked mobile robot," in *2008 IEEE/RSJ International Conference on Intelligent Robots and Systems*, 2008, pp. 95–100.

[19] V. Rajagopalan, Ç. Meriçli, and A. Kelly, "Slip-aware model predictive optimal control for path following," in *2016 IEEE International Conference on Robotics and Automation*, 2016, pp. 4585–4590.

[20] J. Yi, D. Song *et al.*, "Adaptive trajectory tracking control of skid-steered mobile robots," in *Proceedings 2007 IEEE International Conference on Robotics and Automation*. IEEE, 2007, pp. 2605–2610.

[21] E. Panteley, A. Loria, and A. Teel, "Relaxed persistency of excitation for uniform asymptotic stability," *IEEE Transactions on Automatic Control*, vol. 46, no. 12, pp. 1874–1886, 2001.

[22] M. G. Bekker, "Off-the-road locomotion," *Research and development in terramechanics*, 1960.

[23] J. Y. Wong, *Theory of Ground Vehicles*, 4th ed. John Wiley & Sons, 2008.

[24] T. Zou, J. Angeles, and F. Hassani, "Dynamic modeling and trajectory tracking control of unmanned tracked vehicles," *Robotics and Autonomous Systems*, vol. 110, pp. 102 – 111, 2018.

[25] H. K. Khalil, *Nonlinear Systems*, 3rd ed. Prentice Hall, 2002.

[26] R. Tazzari, D. Mengoli, and L. Marconi, "Design Concept and Modelling of a Tracked UGV for Orchard Precision Agriculture," in *2020 IEEE International Workshop on Metrology for Agriculture and Forestry (MetroAgriFor)*, 2020, pp. 207–212.